

A CENSUS OF BARYONS IN GALAXY CLUSTERS AND GROUPS

ANTHONY H. GONZALEZ¹, DENNIS ZARITSKY^{2,3}, & ANN I. ZABLUDOFF^{2,3}

To appear in The Astrophysical Journal

ABSTRACT

We determine the contribution of stars in galaxies, intracluster stars, and the intracluster medium to the total baryon budget in nearby galaxy clusters and groups. We find that the baryon mass fraction ($f_b \equiv \Omega_b/\Omega_m$) within r_{500} is constant for systems with \mathcal{M}_{500} between $6 \times 10^{13} M_\odot$ and $1 \times 10^{15} M_\odot$. Although f_b is lower than the WMAP value, the shortfall is on the order of both the observational systematic uncertainties and the depletion of baryons within r_{500} that is predicted by simulations. The data therefore provide no compelling evidence for undetected baryonic components, particularly any that would be expected to vary in importance with cluster mass. A unique feature of the current analysis is direct inclusion of the contribution of intracluster light (ICL) in the baryon budget. With the addition of the ICL to the stellar mass in galaxies, the increase in X-ray gas mass fraction with increasing total mass is entirely accounted for by a decrease in the total stellar mass fraction, supporting the argument that the behavior of both the stellar and X-ray gas components is dominated by a decrease in star formation efficiency in more massive environments. Within just the stellar component, the fraction of the total stellar luminosity in the central, giant brightest cluster galaxy (BCG) and ICL (hereafter the BCG+ICL component) decreases as velocity dispersion (σ) increases for systems with $145 \text{ km s}^{-1} \leq \sigma \leq 1026 \text{ km s}^{-1}$, suggesting that the BCG+ICL component, and in particular the dominant ICL component, grows less efficiently in higher mass environments. The degree to which this behavior arises from our sample selection, which favored systems with central, giant elliptical galaxies, remains unclear. A more robust result is the identification of low mass groups with large BCG+ICL components, demonstrating that the creation of “intracluster” stars does not require a massive cluster environment. Within r_{500} and r_{200} , the BCG+ICL contributes on average 40% and 33% of the total stellar light, respectively, for the clusters and groups in our sample. Because these fractions are functions of both enclosed radius and system mass, care should be exercised when comparing these values with other studies and simulations.

Subject headings: galaxies: clusters: general — galaxies:cD, formation, evolution, fundamental parameters

1. INTRODUCTION

An important step in understanding any astrophysical system is a full accounting of its constituent components. Over scales ranging from groups to clusters of galaxies, measuring how baryons are distributed among their various gaseous and stellar phases can provide clues to the roles played by AGN feedback, starburst winds, galaxy mergers, and tidal stripping (Merritt 1984; Roussel et al. 2000; Valdarnini 2003; De Lucia et al. 2004; Kravtsov et al. 2005; Cheng et al. 2005; Ettori et al. 2006; Monaco et al. 2006) in driving galaxy evolution in these complex environments. Determining the total contribution of these baryonic components to the cluster mass is similarly valuable. While the baryon fraction in clusters may be expected to reflect the universal value (see White et al. 1993; Ettori et al. 2006), baryon accountings in clusters to date have fallen short of this expectation (Ettori 2003; McCarthy et al. 2006) and uncovered possible intriguing trends with cluster mass (Lin et al. 2003). With the precise measurement of the universal baryon fraction from WMAP ($f_b \equiv \Omega_b/\Omega_m = 0.176_{-0.013}^{+0.008}$; Spergel et al. 2006), this shortfall has gained in physical significance,

leading to suggestions that physical processes lower the cluster baryon fraction relative to the Universe (see, for example, He et al. 2005), that there may be significant, undetected baryon components (see Ettori 2003; Lin & Mohr 2004), or that WMAP underestimates Ω_m (McCarthy et al. 2006). Any investigation along these lines first requires measurement of *all* the baryon components, including the hot, X-ray emitting gas and the stars in and out of galaxies.

One baryonic component that past studies were unable to include directly is the intracluster stars (hereafter the intracluster light or ICL). In recent years, multiple studies have detected intracluster light via stacking of large cluster samples (Zibetti et al. 2005), deep observations of individual clusters (Feldmeier et al. 2004b; Gonzalez et al. 2005; Krick et al. 2006), and even identification of *individual* intracluster stars in very nearby clusters (Durrell et al. 2002; Feldmeier et al. 2004a; Aguerri et al. 2005; Ciardullo et al. 2005; Gerhard et al. 2005). The general consensus is now that all clusters have an ICL component. The natural extension of these studies is placing the ICL in the larger context of cluster and group evolution, examining directly whether this component is important in the chemical enrichment of the intragalactic medium (Lin & Mohr 2004; Zaritsky et al. 2004), the total stellar budget, or even in the total baryon budget. While recent work suggests that the ICL does not contribute much to the overall baryon budget of the

¹ Department of Astronomy, University of Florida, Gainesville, FL 32611-2055

² Steward Observatory, University of Arizona, 933 North Cherry Avenue, Tucson, AZ 85721

³ Center for Cosmology and Particle Physics, Dept. of Physics, NYU, New York, NY, 10003

most massive clusters (the ones most often observed), it could become important in lower mass systems where the plasma is less dominant and the apparent discrepancy between observations and the WMAP baryon fraction is most severe (e.g. Lin et al. 2003). This issue is mostly unexplored, as previous ICL measurements have come either from a few systems with little dynamic range (Feldmeier et al. 2004a; Krick et al. 2006) or from stacked systems for which mass estimators have been crude (Zibetti et al. 2005).

In our program we include the ICL’s contribution to the total baryon mass budget directly, explore the dependence of total baryon fraction on cluster mass, and consider the relative importance of the stars in the ICL to those in galaxies and of the total stellar mass to the total gas mass in the intracluster medium (ICM). We focus on a sample of 23 nearby galaxy clusters and groups with ICL measurements from Gonzalez et al. (2005) that span a wide range in velocity dispersion, $145 \text{ km s}^{-1} \leq \sigma \leq 1026 \text{ km s}^{-1}$. We determine the cluster radii and masses at an overdensity of 500 times critical density (r_{500} and \mathcal{M}_{500} ; §3.1), revisit our previous ICL measurements (§3.2), measure the total luminosity in the cluster galaxies (§3.3), determine stellar masses (§3.4), and obtain gas masses from the literature (§3.5). We then derive relationships for the stellar and total baryon mass fraction with cluster mass (§4.1), examine the detailed behavior of the ICL relative to the galaxy luminosity (§4.2), and speculate about the origin of the observed trends (§4.3). Throughout this paper we assume a cosmology with $\Omega_M = 0.27$, $\Omega_\Lambda = 0.73$, and $H_0 = 70 \text{ km s}^{-1}$.

2. SAMPLE DEFINITION AND DATA

In Paper I (Gonzalez et al. 2005), we present a sample of 24 clusters and groups for which we obtained drift scan imaging in Gunn i using the Great Circle Camera (Zaritsky et al. 1996) on the Las Campanas 1m Swope telescope. The sample is comprised of systems at $0.03 < z < 0.13$ that contain a dominant brightest cluster galaxy (BCG) with a major axis position that lies within 45° of the direction of the drift scan, east-west, and span a range of velocity dispersions and Bautz-Morgan types (Bautz & Morgan 1970). We refer the reader to Paper I for further details concerning the data and photometric reductions.

In Paper II (Zaritsky et al. 2006), we present velocity dispersions for 23 of these clusters and groups. Twelve of these σ ’s are based on our own observations with the Hydra spectrograph at the CTIO Blanco 4m telescope, while the rest are derived from galaxy redshifts in the literature. For all but four systems, the velocity dispersions are calculated using > 20 confirmed members within 1.5 Mpc of the BCG. The system with the smallest number of confirmed members has 8 galaxies and the lowest σ ($144_{-57}^{+78} \text{ km s}^{-1}$). Details of the spectroscopic reductions and velocity dispersion measurements are given in Paper II. The information from both Papers I and II relevant to the current analysis is presented in Table 1. The magnitudes in this Table do not include extinction or k-corrections, which are listed in a separate column. When converting to stellar masses in §3.4 we do include these corrections.

3. ANALYSIS

To determine the ratio of baryons to total mass for each group and cluster in our sample, we 1) estimate the total masses and cluster radii, 2) calculate the combined luminosity of the brightest cluster galaxy and intracluster light, 3) determine the total luminosity associated with the other cluster members, 4) convert the luminosities of these components into stellar masses, and 5) obtain X-ray gas mass fractions from the literature. In §4, we discuss the relationships between total system mass and stellar mass, X-ray gas mass, and total baryon mass.

3.1. Cluster Radii and Masses

To estimate the total baryon fraction from the stellar components and ICM, we must first choose a fixed radius within which the baryons can be summed and then determine the baryonic and total masses within this radius. We choose r_{500} , the radius at which the cluster mass density exceeds the critical value by a factor of 500, and the largest radius for which the current X-ray data require no model extrapolation (Vikhlinin et al. 2006). Measurements of the ICL typically do not extend even out to r_{500} , but the light is sufficiently concentrated within a few hundred kpc that the model extrapolation to r_{500} introduces a minimal uncertainty.

The systems in our ICL sample have measured velocity dispersions, but generally lack X-ray data. To obtain r_{500} and \mathcal{M}_{500} values for the clusters in our ICL sample that are directly comparable to those determined in X-ray studies, we therefore derive calibrations of the σ - r_{500} and σ - \mathcal{M}_{500} relations using the clusters from Vikhlinin et al. (2006) that also have published velocity dispersions (Girardi et al. 1998; Wu et al. 1999). The fit to the σ - r_{500} relation has a slope consistent with the theoretical expectation (1.07 ± 0.12 vs 1) and corresponds to a cluster with $\sigma = 1000 \text{ km s}^{-1}$ having an r_{500} of 1.41 Mpc. The best fit to the σ - \mathcal{M}_{500} relationship using the Vikhlinin et al. (2006) sample has a slope consistent with the theoretical expectation (3.37 ± 0.53 vs. 3) and corresponds to a cluster with $\sigma = 1000 \text{ km s}^{-1}$ having an enclosed mass, \mathcal{M}_{500} , of $7.6 \times 10^{14} M_\odot$. A similar analysis can be performed for r_{200} using the sample of Arnaud et al. (2005), but with the limitation that only five clusters in this sample have published velocity dispersions. Fixing the slope to the value derived for the Vikhlinin et al. (2006) sample, the resulting normalization yields an r_{200} of 2.2 Mpc for a $\sigma = 1000 \text{ km s}^{-1}$. We utilize this r_{200} relation in §4.2.3 when quantifying the radial dependence of the ICL.

For comparison, we also derive r_{500} and r_{200} using the approach of Hansen et al. (2005), directly calculating the radius within which the number density of cluster galaxies implies that the mass density exceeds the critical value by a factor of 200 or 500. If the bias between the galaxy distribution and dark matter is not large, this approach is expected to yield a reasonable estimate for these radii. As in Hansen et al. (2005), we use the Blanton et al. (2003) SDSS i -band luminosity function integrated over redshift to compute the field density (see Hansen et al. 2005). When computing r_{200} and r_{500} , we impose a faint magnitude limit of $m_I = 18$; varying this limit by ± 0.5 mag alters the derived r_{200} values by $\pm 5\%$. We find that two approaches yield consistent values ex-

TABLE 1
CLUSTER SAMPLE

Cluster	BM Type	$\langle z \rangle$	σ (km s^{-1})	$\log \mathcal{M}_{500}$ (M_{\odot})	$M_{BCG+ICL,r_{500}}$ ^{ab} (mag)	$M_{gal,r_{500}}$ ^c (mag)	e+k Correction ^d (mag)	BCG+ICL Fraction < r_{500}
Abell 0122	I	.1134	677^{+108}_{-94}	14.31	-25.60 ± 0.04	-26.11	0.12	$0.38 \pm .04$
Abell 1651	I-II	.0847	990^{+112}_{-101}	14.87	-25.63 ± 0.10	-26.88	0.13	$0.24 \pm .04$
Abell 2400	II	.0880	653^{+62}_{-57}	14.26	-25.08 ± 0.06	-26.10	0.14	$0.28 \pm .06$
Abell 2401	II	.0571	459^{+101}_{-83}	13.74	-24.61 ± 0.03	-25.57	0.09	$0.29 \pm .03$
Abell 2405 ^{e,f}		.0368	145^{+78}_{-57}	12.05	-23.68 ± 0.14	-21.24	0.11	$0.90 \pm .14$
Abell 2571	II	.1091	671^{+83}_{-74}	14.30	-25.37 ± 0.10	-25.53	0.16	$0.46 \pm .10$
Abell 2721	II	.1144	842^{+81}_{-74}	14.63	-25.19 ± 0.02	-26.90	0.12	$0.17 \pm .02$
Abell 2730	II	.1201	1021^{+154}_{-135}	14.91	-26.04 ± 0.11	-26.49	0.11	$0.40 \pm .11$
Abell 2811	I-II	.1079	860^{+114}_{-141}	14.66	-25.64 ± 0.08	-26.40	0.11	$0.33 \pm .08$
Abell 2955	II	.0943	316^{+85}_{-67}	13.19	-25.16 ± 0.06	-24.96	0.11	$0.55 \pm .06$
Abell 2969	I	.1259	982^{+192}_{-161}	14.85	-25.58 ± 0.08	-26.62	0.13	$0.28 \pm .08$
Abell 2984	I	.1042	490^{+112}_{-91}	13.84	-25.63 ± 0.05	-25.51	0.11	$0.53 \pm .05$
Abell 3112	I	.0753	941^{+139}_{-121}	14.79	-25.76 ± 0.03	-26.96	0.08	$0.25 \pm .03$
Abell 3166	I	.1174	205^{+43}_{-36}	12.56	-24.55 ± 0.06	-23.99	0.10	$0.63 \pm .06$
Abell 3693 ^f		.1229	1026^{+149}_{-130}	14.92	-25.49 ± 0.05	-26.65	0.12	$0.26 \pm .05$
Abell 3705	III	.0895	1009^{+81}_{-75}	14.89	-24.37 ± 0.02	-26.53	0.15	$0.12 \pm .02$
Abell 3727	III	.1159	582^{+114}_{-95}	14.09	-24.97 ± 0.06	-25.83	0.24	$0.31 \pm .06$
Abell 3809	III	.0623	544^{+55}_{-50}	13.99	-24.69 ± 0.04	-25.38	0.08	$0.35 \pm .04$
Abell 3920	I-II	.1268	426^{+136}_{-103}	13.63	-25.06 ± 0.04	-25.27	0.12	$0.45 \pm .04$
Abell 4010	I-II	.0955	634^{+145}_{-118}	14.21	-25.56 ± 0.08	-26.25	0.11	$0.35 \pm .08$
APMC 020 ^f		.1098	242^{+57}_{-47}	12.80	-24.87 ± 0.09	-23.55	0.11	$0.77 \pm .09$
Abell S0084	I	.1080	522^{+155}_{-122}	13.93	-25.38 ± 0.04	-26.16	0.12	$0.33 \pm .04$
Abell S0296	I	.0696	477^{+76}_{-65}	13.80	-25.19 ± 0.04	-25.17	0.09	$0.51 \pm .04$

NOTE. — The quoted uncertainties include the systematic uncertainties associated with the BCG+ICL luminosities due to sky subtraction, the background subtraction for the galaxy luminosity, and the uncertainty in the faint end slope of the cluster galaxy luminosity function.

^aFor both the BCG+ICL and galaxies, the quoted absolute magnitudes do *not* include the corrections for extinction or k-dimming listed in column 8.

^cThe estimated uncertainty for the galaxies is 0.15 mag.

^dThe extinction corrections are based upon the Schlegel et al. (1998) dust maps and the k-corrections assume a passive stellar population.

^eAbell 2405 is a superposition of two relatively poor systems at 11,000 and 27,000 km s^{-1} . While this superposition hinders a robust measurement for the luminosity of the cluster galaxies, the BCG+ICL fraction is $> 80\%$ within r_{500} even if no galaxy background subtraction is performed.

^fNo published Bautz-Morgan type. Abell 2405 and Abell 3693 each have two discrete redshift peaks. Published Bautz-Morgan types do exist for these clusters, but not for the redshift peaks that we are studying.

cept for clusters with low velocity dispersions ($\lesssim 400 \text{ km s}^{-1}$), where the Hansen et al. (2005) approach yields larger radii (by as much as a factor of two). For all analyses below we use the X-ray derived values; no results in the paper change qualitatively if we instead use the values from the Hansen et al. (2005) approach.

3.2. Total Luminosity of BCG+ICL

A key question in previous discussions of these data (Zaritsky et al. 2004; Gonzalez et al. 2005) was whether the BCG and ICL are distinct entities. A central result of Paper I is that the stellar surface brightness, position angle, and ellipticity profiles of these clusters are best reproduced when the BCG and ICL are fit as separate components. In this analysis we choose to combine the luminosity of these two components and refer to the combined entity as simply the BCG+ICL. There are several strong motivations for this choice in the current context. Observationally, the separation of the two components is difficult and the combined luminosity is therefore a more robust quantity than the luminosity of either sep-

arately. Using the combined quantity also avoids choosing among the various ICL definitions in the literature (e.g., Feldmeier et al. 2004b; Zibetti et al. 2005), enabling a more straightforward comparison between our results and other observational studies and simulations. Lastly, because we are interested here in a full baryon accounting, the question of whether they reside in the central galaxy or in intracluster space is not as critical as in other contexts. In later discussions of the ICL relative to the galaxy luminosities (§4.2), where the distinction between BCG and ICL is relevant, we reiterate from Paper I that the bulk ($> 80\%$) of the luminosity in the cluster's BCG+ICL is contained in the ICL.

We determine the luminosity of the BCG+ICL component as follows. In Paper I we used the GALFIT package (Peng et al. 2002) to fit the surface brightness distribution in each cluster out to a radius of 300 kpc from the BCG. The BCG and ICL were best fit with separate $r^{1/4}$ profiles. Here we use those best-fit profiles to construct a 2-D model image from which we determine the flux within circular apertures corresponding to r_{500} (in our

analysis of the baryon mass fraction; §4.1) and to fractions of r_{200} (in our determination of the BCG+ICL’s contribution to the total stellar light; §4.2). We estimate the systematic errors in the measured fluxes using the $\pm 1\sigma$ systematic uncertainties in the structural parameters of the best-fit profiles (these exceed the statistical errors due to uncertainties in the sky level; see Paper I). The advantages of using the models rather than placing apertures on the original data are that we minimize contamination from cluster galaxies, interpolate directly over masked regions, and provide a robust means of quantifying the systematic uncertainties. We use circular rather than elliptical apertures to enable direct comparison with other studies and simulations.

An implicit assumption in this work is that our models from Paper I, which are determined for $r < 300$ kpc, adequately describe the ICL at all radii. In our models, 80% of the total light of the BCG+ICL is contained in the central 300 kpc, making it unlikely that we are significantly overestimating the luminosity of this component with our extrapolation. Moreover, the BCG+ICL dominate the total cluster luminosity within this radius, and for our data the potential bias from inclusion of faint, unresolved cluster galaxies in the ICL is at most a few percent (Gonzalez et al. 2000). Although the uniformity of the profiles within 300 kpc argues that extrapolating is reasonable, we will underestimate the ICL luminosity if there is any significant contribution at larger radii that is not included in our model. We expect that the best method of testing this assumption is via extension of current planetary nebulae studies in nearby clusters like Virgo (Feldmeier et al. 2004a) to large fractions of r_{200} . Because of the nature of this study, we are most concerned with overestimating the ICL, and large overestimates ($> 30\%$) are not possible.

3.3. Total Luminosity of Cluster Galaxies

We compute the total luminosity of non-BCG cluster galaxies within the same apertures (r_{500} and fractions of r_{200}) used for the BCG+ICL. Hereafter, we refer to the non-BCG cluster galaxies as simply “cluster galaxies”. After excluding stars using the SExtractor (Bertin & Arnouts 1996) stellerity index, we sum the flux of all galaxies fainter than the BCG and brighter than $m_I = 18$ lying within the aperture. We then perform a statistical background subtraction, and include a completeness correction to account for the contribution of fainter cluster members (see below). In cases where the aperture size is larger than the width of the drift scan images, we also apply a correction to account for the lost area. Specifically, we weight the luminosity contribution of each galaxy by the inverse of the fractional area lost at that radius (e.g., a galaxy would have a weighting factor of two if half the area is lost).

Because the determination of the flux density from background galaxies is critical in this type of measurement, we estimate the background using two independent methods. First, we compute the background galaxy density with an annular region located $30'$ to $60'$ from the BCG. This method, which was also used in Paper I, has the advantage that the photometry for the background and cluster galaxies is performed in the same fashion from the same images. However, large scale structure may bias the observed background level even

at these large radii. To ascertain whether we are suffering from such a bias, we also compute the background level using the Sloan Digital Sky Survey luminosity function from Blanton et al. (2003), integrating over redshift and applying mean evolutionary and k-corrections derived from Bruzual & Charlot (2003) models with the Padova isochrones (Bertelli et al. 1994). A comparison of the results from the two techniques shows that for the ensemble of systems the total cluster galaxy luminosities after background subtraction are consistent to within 10%. In the subsequent discussion, we apply the first method of direct background subtraction because this approach relies on fewer assumptions.

After background subtraction, we include a completeness correction to account for the luminosity contribution from cluster members fainter than the limiting magnitude. For this correction, we adopt the cluster luminosity function of Christlein & Zabludoff (2003), $\alpha = -1.21$ and $M_{*,R} = -21.14$, using $R - I = 0.82$ to convert from R to I . Although the value of M_* is identical to the i -band value for the field from Blanton et al. (2003), the cluster luminosity function has a slightly steeper faint end slope. Using a different value of α systematically shifts the total luminosity due to cluster galaxies and thus the total stellar light of the cluster. For $\alpha = -1$, the computed total luminosity of the cluster galaxies would on average be 12% lower, increasing the relative importance of the BCG+ICL, but decreasing the stellar contribution to the overall baryon budget. The total luminosities of the BCG+ICL and of the cluster galaxy components are presented in Table 1.

3.4. Total Stellar Masses

The conversion from luminosity to stellar mass for the cluster galaxies and the BCG+ICL potentially incurs the most significant uncertainty in the total baryon mass budget. A straightforward theoretical calculation, based on PEGASE2.0 (Fioc & Rocca-Volmerange 1997) for a Salpeter IMF and a 10 Gyr old population, yields $M/L_I = 4.7$, but recent observations indicate that real systems exhibit lower M/L . To estimate a mean M/L , we use the SAURON results from Cappellari et al. (2006), which provide an empirical determination of the central stellar M/L using Schwarzschild dynamical modeling of two-dimensional kinematic data. Equation 9 in Cappellari et al. (2006) provides the luminosity dependence of the mass-to-light ratio in the I -band. We compute a luminosity-weighted M/L for $L > 0.25L_*$ (the range over which the SAURON relation is determined) using the same Christlein & Zabludoff (2003) luminosity function as in §3.3. We adopt the resultant value, $M/L = 3.6$, for both the cluster galaxies and the BCG+ICL in our baryon calculation, but note that the uncertainty is at least 10% and that M/L varies with both mass (Cappellari et al. 2006; Zaritsky et al. 2006) and stellar population. An improved accounting for the ICL component would require knowledge of the source of the ICL stars if the variations in M/L are driven by population, rather than dynamical, differences. An improved accounting for the cluster galaxy population would require determining the fraction of spiral galaxies in these clusters and using a more appropriate M/L for the spirals.

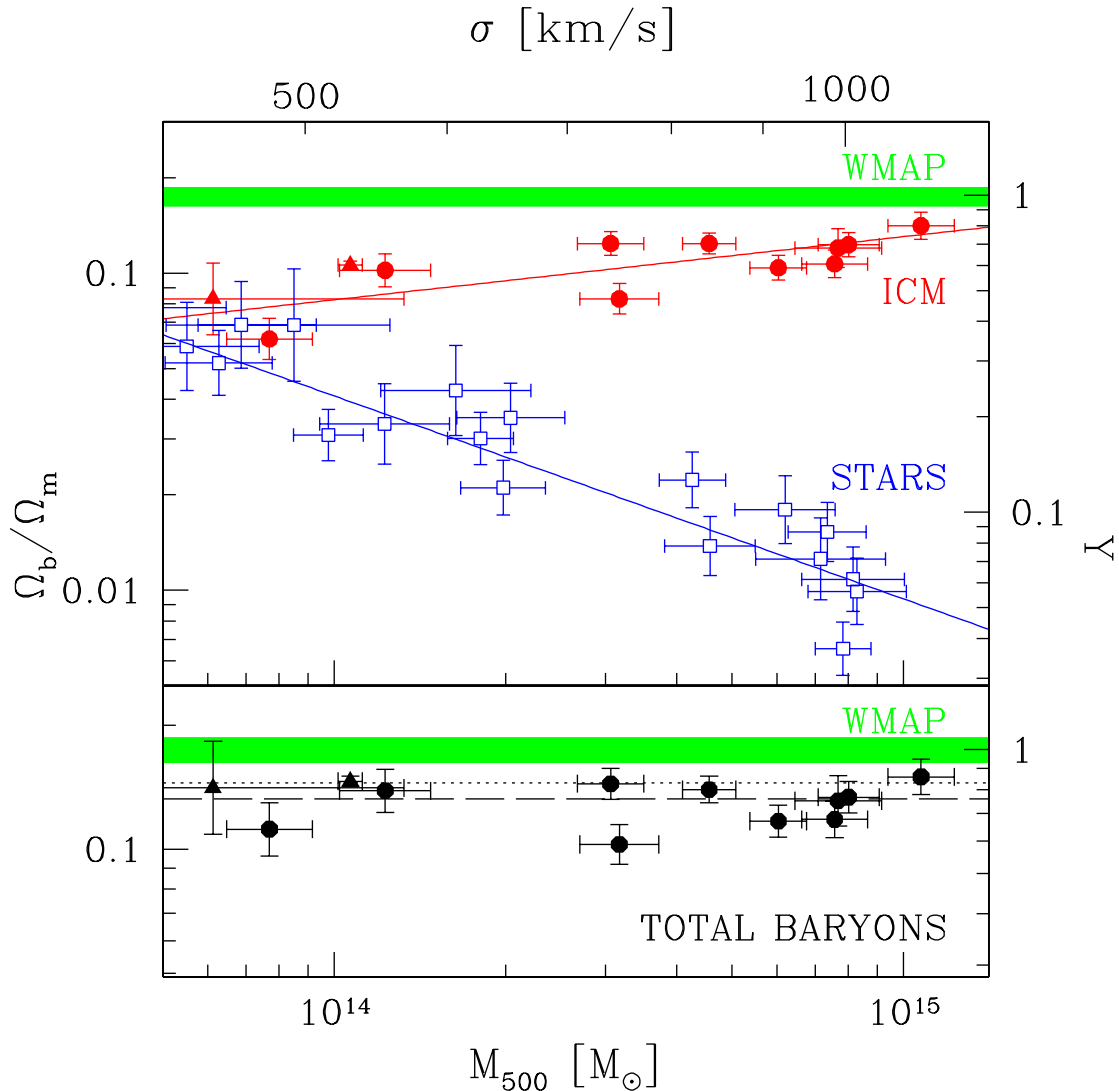


FIG. 1.— Determination of cluster and group baryon fractions within r_{500} as a function of \mathcal{M}_{500} (bottom axis) and velocity dispersion (top axis). Plotted are X-ray gas mass fractions from Vikhlinin et al. (2006) (filled circles) and Gastaldello et al. (2006) (filled triangles), and the stellar mass fractions (BCG+ICL+galaxies, open squares) for systems in our sample with masses that overlap the range shown for the X-ray studies. All measurements are within r_{500} . Overplotted are the best fit relations for the Vikhlinin et al. (2006) sample gas mass fractions and for our stellar mass fractions. The WMAP 1σ confidence region for the universal baryon fraction from Spergel et al. (2006) is shown for comparison, and the right-hand axis shows Y , the ratio of the baryon fraction for each component to the universal value from WMAP. *Lower panel:* The total baryon fraction derived for the Vikhlinin et al. (2006) and Gastaldello et al. (2006) clusters if our best-fit stellar baryon relation is used to estimate a stellar baryon contribution for each of these systems. The weighted mean for the sample (dashed line) is $\Omega_b/\Omega_m = 0.133 \pm 0.004$. We observe no trend in baryon fraction with cluster mass. The error bars on the individual data points and the weighted mean include only statistical uncertainties. The unweighted mean for the combined Zhang et al. (2007) and Rasmussen & Ponman (2006) samples (dotted line) is included to provide a sense of the systematic uncertainties.

3.5. Total Mass in the Intracluster Medium

Determination of total cluster baryon fractions also requires measurement of the mass of hot gas in the intracluster medium. Because we lack these data for clusters in our sample, in §4 we fit the behavior of the stellar mass fraction with cluster mass and use this relation to derive total baryon fractions for clusters with published X-ray gas fractions. For the gas mass fractions we adopt the values of X-ray gas fraction inside of r_{500} , f_g , and of enclosed mass, \mathcal{M}_{500} , from the tabulations by Vikhlinin et al. (2006) and Gastaldello et al. (2006). The

latter adds only two new systems, but helps constrain the baryon fraction at low mass. We note that there are several systems for which the X-ray gas fraction was measured by both groups. In these instances there is reasonably good agreement, and hence we expect no significant relative systematic biases between the two samples.

4. RESULTS AND DISCUSSION

4.1. Baryon Mass Fraction versus Cluster Mass

In this section, we obtain two principal results. First, summing the three baryonic components — the hot gas

of the intracluster medium, the stars of the BCG+ICL, and the stars of the other cluster galaxies — gives a total baryon mass fraction, f_b , that is constant as a function of total mass (Figure 1). This constancy contradicts previous studies and arises in large part from the inclusion of the ICL for systems with $\mathcal{M}_{500} < \text{few} \times 10^{14} M_\odot$. Second, the weighted mean value of the total baryon mass fraction is $f_b = 0.133$.⁴ For reasons discussed below, we conclude that there is no compelling case for undetected baryons in the groups and clusters in our sample.

We fit the behavior of the stellar and X-ray gas mass fractions with mass as power laws (top panel of Figure 1). Within r_{500} , the stars result in a relationship $\log(f_*) = (7.57 \pm 0.08) - (0.64 \pm 0.13) \log(\mathcal{M}_{500})$ and the plasma in $\log(f_g) = (-3.87 \pm 0.04) + (0.20 \pm 0.05) \log(\mathcal{M}_{500})$ for the sample of Vikhlinin et al. (2006).⁵ The behavior of the two components is clearly inverted. The plasma component, which dominates at cluster masses $> 10^{14} M_\odot$, has a shallower dependence on mass than the stellar component. We use our best fit relation for the stellar mass to convert the X-ray gas fractions from Vikhlinin et al. (2006) and Gastaldello et al. (2006) to total baryon fractions on a cluster-by-cluster basis. The resulting total baryon fractions, shown in the lower panel of Figure 1, are independent of cluster mass over the range of \mathcal{M}_{500} from 6×10^{13} to $10^{15} M_\odot$. If one considers only the statistical uncertainties associated with our total cluster baryon fraction and the WMAP measurement, then the two values are discrepant at the level of 3.2σ .

There are three possible interpretations of this result in the context of a full baryon accounting. First, systematic uncertainties may be significantly larger than the random errors, and our measurement may therefore be consistent with the universal WMAP value. Because the gas mass fraction is much larger than the stellar mass fraction over the majority of the mass range we probe, we focus this discussion on potential errors in the gas mass fraction. Systematic errors, by their nature, are often difficult to calculate and can best be illuminated by comparing independent studies. Zhang et al. (2007) and Rasmussen & Ponman (2006) provide gas mass fractions for high and low mass systems, respectively. Zhang et al. (2007) find gas fractions that are 15% larger than those we adopted over the range probed by their sample. Rasmussen & Ponman (2006) also find gas fractions that are larger than those we adopted for comparably low mass systems. Together, these two samples cover the mass range of our adopted sample and result in an average $f_b = 0.149$, which is 2.1σ discrepant with the WMAP value and 12% larger than the f_b we derive for the Vikhlinin et al. (2006) data set. We conclude that indeed the systematic uncertainties dominate, that the sense of the uncertainty works to diminish the discrepancy between measurements and expectations, and that the case for undetected baryon components rests on removing these systematic uncertainties. Second, the baryon mass fraction with r_{500} in clusters may be different from the universal value. Clus-

ter simulations routinely predict baryon fractions that are lower than the universal baryon fraction by $\sim 10\%$. We have deliberately not adopted any of those as the target because there are still a minority of simulations that predict a baryon fraction larger than universal (e.g. Kravtsov et al. 2005). Third, the shortfall may be resolved by yet undetected baryon components. The constancy of the measured baryon fraction with total system mass argues against a large undetected component, but one could contribute at a modest level and bypass current detection. In the end, all of these possibilities may contribute at some level to a final resolution of the baryon accounting, but at this point we are left to conclude that there is no compelling evidence for undetected baryons.

We close this section by comparing our study to that of Lin et al. (2003), who obtained a dependence of the baryon fraction on cluster mass in conflict with our result. The range of masses covered by the two studies is the same, and we both use r_{500} as our fiducial radius, so the discrepancy is real. The most obvious differences are our inclusion of the ICL component and our different normalization of the gaseous component. We model the effect of including the ICL into their accounting by using our relationship for the BCG+ICL mass vs. system mass and “correcting” their values of the baryon fraction on a cluster-by-cluster basis.⁶ The relationship between baryon fraction and mass decreases from a $\sim 3\sigma$ result in the original Lin et al. (2003) study to a 1.8σ result in the corrected case. Therefore, the inclusion of the ICL explains part of the discrepancy between our result and that of Lin et al. (2003), although apparently not all of it. The lack of the ICL in the Lin et al. (2003) accounting was not an oversight — they attempted to model the effect of the ICL in Lin & Mohr (2004), but simply lacked data of the sort we present here. While the exclusion of the ICL causes a relative underprediction of the contribution of stellar baryons for the lowest mass systems, the Lin et al. adopted X-ray gas fractions, which are $\sim 25\%$ larger than ours and hence consistent with the WMAP baryon mass fraction for the most massive systems, cause a relative overprediction of baryons in the highest mass systems. These two effects lead to the apparent mass-dependent baryon fraction of Lin et al. As with the comparison among different studies discussed previously, we have an unresolved discrepancy in the gas mass fractions at the $\sim 20\%$ level that highlights the difficulty in such an analysis and supports our contention that there is yet no compelling evidence for either additional baryonic components or a trend in baryon fraction with system mass.

4.2. Stellar Component of Clusters and Groups

4.2.1. Behavior vs. \mathcal{M}_{500}

We now consider the behavior of the stellar component in more detail. We compute the dependence of the optical luminosity on \mathcal{M}_{500} for the cluster galaxies, the BCG+ICL, and the sum of these populations. There are multiple studies of the dependence of the total stellar luminosity of cluster galaxies on cluster mass. In the K -band, Lin et al. (2004) find that for the galaxies alone (excluding the BCG) $L \propto M^\gamma$ with $\gamma = 0.82 \pm 0.05$

⁴ Defining Y to be the ratio of the baryon fraction to the cosmic value from the WMAP third year results, this value for the total baryon fraction corresponds to $Y = 0.76$.

⁵ Note that while this fit applies only to the Vikhlinin et al. (2006) data set, the Gastaldello et al. (2006) points in Figure 1 are consistent with this relation.

⁶ This is a slight ($\sim 20\%$) overcorrection because it includes the BCG, which Lin et al. (2003) had already included.

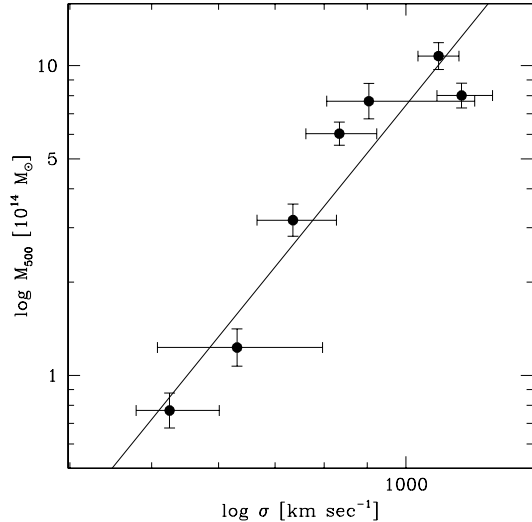


FIG. 2.— Calibration of velocity dispersion to X-ray derived masses within r_{500} . We plot the seven systems from Vikhlinin et al. (2006) for which we found velocity dispersions in the literature (Girardi et al. 1998; Wu et al. 1999). The line is our fit to the data, and hence our calibration for converting the velocity dispersions measured for our optical clusters into M_{500} 's.

($\gamma = 0.82 \pm 0.04$) within r_{500} (r_{200}), and Ramella et al. (2004) find $\gamma = 0.74 \pm 0.06$ within r_{200} . A least-squares fit to our I -band data for the cluster galaxies yields $\gamma = 0.71 \pm 0.07$ within r_{500} , which is consistent with these results and most other published values (Girardi et al. 2000; Rines et al. 2004, but see Kochanek et al. (2003) for an exception). We conclude that the conflict between our result — that the baryon mass fraction is insensitive to system mass for groups and clusters — and those of past studies does not arise predominantly from our measurement of cluster galaxy properties.

In comparison with the cluster galaxy luminosity versus cluster mass relation, the correlation between BCG+ICL luminosity and cluster mass is weaker, increasing by only about a factor of two in total luminosity between poor groups with $\sigma = 400 \text{ km s}^{-1}$ and rich clusters with $\sigma = 1000 \text{ km s}^{-1}$ (Figure 3). The existence of groups in which the fraction of stars in the BCG+ICL exceeds that in galaxies out to r_{500} (Figure 4) demonstrates that the rich cluster environment is not a requirement for the production of a significant intracluster stellar population. Instead, it appears that local density maxima in both the group and cluster environments are capable of generating intracluster stars, presumably via tidal processes. This conclusion is valid whether one is interested in the combination of the BCG and ICL, or in the ICL alone, because the latter contains the bulk (typically $> 80\%$) of the total light in the two components (Gonzalez et al. 2005). However, our results should not be interpreted to mean that all groups have a significant ICL component, because our original sample selection focused on systems with dominant BCGs.

The observed weak dependence in the BCG+ICL is given by $\gamma = 0.39 \pm 0.05$. Physically, this result implies that production of the BCG+ICL — presumably from the stripping of stars from galaxies — is more efficient in group (or subcluster) environments than in clus-

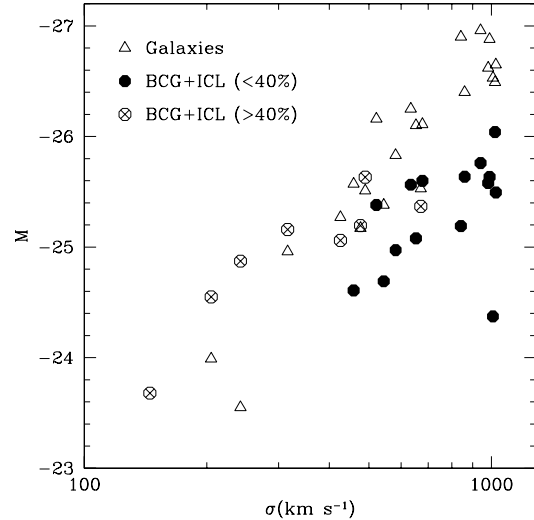


FIG. 3.— The total absolute magnitude of the BCG+ICL component (circles) and of cluster galaxies (triangles) within r_{500} as a function of cluster velocity dispersion. The filled circles denote systems where the BCG+ICL contributes less than 40% of the total luminosity within this radius, while open-crossed circles correspond to systems with higher fractions of light in the BCG+ICL. The BCG+ICL luminosity depends less strongly on the velocity dispersion than does the total galaxy luminosity. We also note that there is no systematic difference in the BCG+ICL absolute magnitudes for clusters with high and low BCG+ICL fractions. The BCG+ICL fraction differences are instead driven predominantly by variations in the total absolute magnitudes of the non-BCG cluster galaxy populations.

ters. Again, we caution that when selecting clusters and groups for this sample, we specifically targeted systems with dominant BCGs. If there is a strong correlation between the presence of a dominant BCG (i.e., our sample) and the total BCG+ICL luminosity (which is not necessarily the case because the ICL contributes much more light), then our selection criteria would artificially produce a smaller γ than that actually found in nature.

4.2.2. Total Cluster Luminosities and Mass-to-Light Ratios

The observed weak dependence of the BCG+ICL luminosity on cluster mass, if real, implies that γ for the total stellar light within r_{500} (L_{500}) must be smaller than the value for the galaxy population alone. The best fit value for the behavior of L_{500} is $\gamma = 0.47 \pm 0.05$, with a scatter of only 0.26 mag about the best fit. Recasting in terms of a mass-to-light ratio yields $M_{500}/L_{500} \propto L_{500}^{1.13 \pm 0.23}$. For comparison, literature values that include only the cluster galaxy contribution typically have $M/L \propto L^{0.3}$. Thus, if the slope we measure for the BCG+ICL component is not significantly biased by our exclusion of groups without a dominant BCG, then our data argue that galaxy cluster mass-to-light ratios are much more strongly dependent upon system mass than is commonly presumed.

Conversely, if our selection against groups lacking a dominant BCG is the reason that the BCG+ICL and cluster galaxy luminosities have different observed cluster mass dependences, then there must exist a correlation between mass-to-light ratio and the presence of a dom-

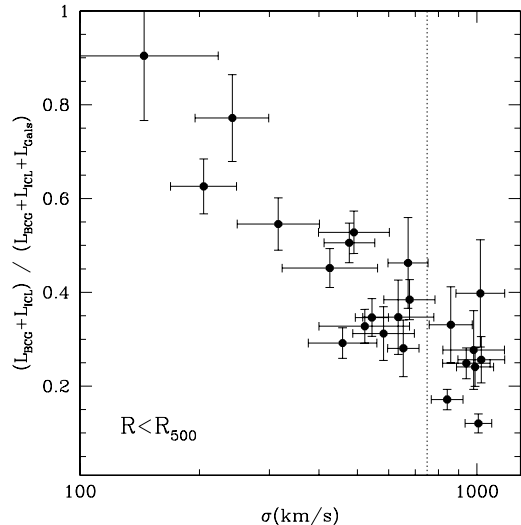


FIG. 4.— The fraction of the total stellar luminosity, measured within r_{500} , which is contained in the BCG+ICL component as a function of cluster velocity dispersion. The dotted vertical line corresponds to $\sigma = 750 \text{ km s}^{-1}$, roughly the median velocity dispersion for an Abell richness class $R \geq 1$ cluster (Zabludoff et al. 1990).

inant BCG. Specifically, for a given velocity dispersion, groups with a dominant BCG have higher BCG+ICL luminosities and hence lower mass-to-light ratios.

4.2.3. BCG+ICL Luminosity Fraction: Dependence on Velocity Dispersion and Radius

We determine the fraction of total stellar luminosity contained in the BCG+ICL component as a function of velocity dispersion and radius. In Figure 4, we plot the BCG+ICL luminosity fraction, $L_{BCG+ICL}/(L_{gal} + L_{BCG+ICL})$ as a function of velocity dispersion within r_{500} , which is slightly larger than the physical region within which the BCG and ICL were modeled in Paper I. We find a trend of decreasing BCG+ICL luminosity fraction with increasing velocity dispersion. The same trend is observed if we use a fixed physical radius of 300 kpc, but the scatter is higher. The presence of this trend is also independent of whether r_{500} or a fixed fraction of r_{200} is used for the abscissa.

Within the clusters, the radial dependence of the BCG+ICL luminosity fraction is shown in Figure 5, where we plot the BCG+ICL luminosity fraction enclosed within different radii. Combining the full ensemble of clusters, the BCG+ICL luminosity fraction decreases smoothly from 65% within $0.1r_{200}$ to 33% within r_{200} . This radial decline, which indicates that the ICL is more concentrated than the galaxies, is also seen by Zibetti et al. (2005) and is predicted by the simulations of Murrante et al. (2004).

Lastly, we use a threshold of $\sigma = 750 \text{ km s}^{-1}$ — roughly the median velocity dispersion of an Abell richness class $R \geq 1$ cluster (Zabludoff et al. 1990) — to divide the data set into two subsamples (Figure 4). The clusters with higher velocity dispersions exhibit lower BCG+ICL luminosity fractions at all radii. To confirm that this result is not driven purely by the BCG, we also compute the corresponding luminosity fractions within

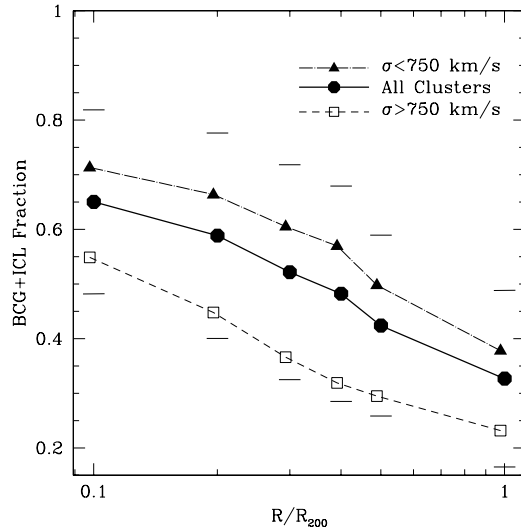


FIG. 5.— The cumulative fraction of light contained in the BCG+ICL as a function of radius. Subdividing the sample into clusters with $\sigma > 750 \text{ km s}^{-1}$ (open boxes) and $\sigma < 750 \text{ km s}^{-1}$ (filled triangles) demonstrates that the BCG+ICL fraction is systematically lower in the more massive clusters. The horizontal dashes included in the plots denote the *rms* variations for the cluster ensemble at each radius.

circular annuli from 0 to $0.5r_{200}$. We find that at all radii the fraction of the cluster luminosity contained in the ICL is lower for the more massive clusters. Moreover, the rms scatter about the mean for the BCG+ICL luminosity fractions is only 10% for the high- σ sample compared with 20% for the low- σ sample within $0.5r_{200}$. Thus, for clusters and groups with a dominant BCG, the BCG+ICL luminosity fractions are smaller and more uniform in the more massive systems.

4.3. Origin of the Baryon Trends

We have identified two independent trends with mass that shed light on the environmental dependencies of physical processes that distribute baryons among the various phases. First, we find that the fraction of stars in the ICL grows (and that in galaxies diminishes) with decreasing system mass. This result is predicated on the assumption that we are not strongly biased in the type of system observed, as discussed above. Even so, we now know that in at least some low mass systems the ICL forms efficiently. As a result, we can rule out cluster-only processes, such as harassment (Moore et al. 1996, 1998), as the dominant ICL formation mechanism, and find support for mechanisms that would be more effective in lower mass systems, such as galaxy-galaxy interactions (Merritt 1984). Such tidal interactions, which could strip stars from galaxies and build up the ICL, are favored in lower mass groups, because the internal velocity dispersions of group galaxies are similar to the velocity dispersion of the group as a whole. If all low mass systems do have high ICL luminosity fractions, and some are the building-blocks of clusters, then a diluting mechanism, such as the infall of individual galaxies into clusters, would be necessary to reduce the final ICL fraction of more massive systems. Of course, it may be that not all low mass groups have high ICL fractions like those in

our sample. The low ICL fractions of high mass clusters may therefore simply reflect their growth by the accretion of groups with lower ICL fractions than we observe. A related possibility is that the clusters accrete and mix progenitor groups before they have time to form substantial ICL via galaxy-galaxy interactions, whereas the ICL continues to grow in more isolated groups. Simulations of the formation of the ICL must reproduce these trends and will lead to a better understanding of the details of the formation mechanisms (Willman et al. 2004; Murante et al. 2004; Sommer-Larsen et al. 2005; Sommer-Larsen 2006; Rudick et al. 2006).

Second, we find that the baryon mass fraction across the range of systems for which we have both optical and X-ray data is roughly constant over the mass range $6 \times 10^{13} M_{\odot} < \mathcal{M}_{500} < 1 \times 10^{15} M_{\odot}$. This result requires a fairly well-tuned balance between the X-ray gas mass fraction, which declines by a factor of two between systems with \mathcal{M}_{500} of $10^{15} M_{\odot}$ and $10^{14} M_{\odot}$, and the stellar mass fraction, which increases by a factor of four to compensate. The matching of the two trends supports the suggestion (Bryan 2000; Lin et al. 2003) that the X-ray gas mass fraction behavior is due to the decreased efficiency of turning gas into stars in the more massive environments. The reduction in star formation efficiency in higher mass systems may arise from the decreased efficiency of tidal interactions among galaxies, the removal of the gaseous reservoirs of galaxies by interactions with the intracluster medium, or increased feedback processes that quench star formation. As usual, interpreting such trends is complicated by the fact that today’s lower mass systems are not necessarily similar to the lower mass antecedents of today’s higher mass systems.

5. CONCLUSIONS

We have conducted a study of 23 nearby galaxy clusters and groups with a dominant, early-type brightest cluster galaxy. For this sample we determine the luminosities of the different stellar constituents (including stars associated with cluster galaxies and the intracluster stars) as a function of cluster velocity dispersion (σ), cluster mass (\mathcal{M}_{500}), and cluster-centric radius. Combining these results with current measurements of the X-ray gas mass as a function of σ , we calculate the dependence of the baryon budget on environment. We reach the following conclusions:

1. The observed total baryon mass fraction within r_{500} is constant for systems with \mathcal{M}_{500} between 6×10^{13} and $10^{15} M_{\odot}$. Although the mean baryon mass fraction is formally $> 3\sigma$ lower than the WMAP measurement, both the observational systematic uncertainties — which dominate the formal random errors — and the predicted deficit of baryons in clusters relative to the universal value are on the order of the observed baryon shortfall. Thus, we conclude that there is no compelling evidence for undetected baryons at this time.

2. The inclusion of the combined light from the brightest cluster galaxy and the intracluster stars, which we refer to as the BCG+ICL component, becomes increasingly important in the baryon budget as the system mass decreases. For systems with $\mathcal{M}_{500} = 10^{14} M_{\odot}$, the BCG+ICL component is nearly 35% of the total stellar luminosity within r_{500} , and the mass of the stellar com-

ponent including the BCG+ICL and the cluster galaxies is comparable to that of the X-ray gas component. Consequently, the increase in X-ray gas mass fraction with increasing \mathcal{M}_{500} is directly reflected by a decrease in the total stellar mass fraction. The matching of the falling stellar mass and rising gas mass with total mass supports the suggestion made previously (Bryan 2000; Lin et al. 2003) that the star formation efficiency decreases with increasing system mass.

3. Considering only the stellar components, we observe that the fraction of the total stellar luminosity in the BCG+ICL decreases with system velocity dispersion. The origin of this trend is that the luminosity of the BCG+ICL component changes more slowly with cluster mass than does the luminosity of cluster galaxies, increasing by only a factor of two between 400 km s^{-1} and 1000 km s^{-1} . The presence of large BCG+ICL luminosity fractions in the lower mass systems demonstrates that the rich cluster environment is not required for production of “intracluster” stars.

The decrease in the importance of the BCG+ICL component, and in particular the dominant ICL component, with increasing cluster mass is consistent with more efficient stripping of stars from galaxies — presumably via galaxy-galaxy interactions — in the lower mass systems. Although it remains unclear the degree to which our sample selection, which favored systems with central, giant elliptical galaxies, impacts this result, it is noteworthy that Purcell et al. (2007) predict precisely the type of relation that we observe using a simple analytic model for BCG+ICL formation from satellite accretion and disruption. A similar model is also able to reproduce the relative luminosities that we observe for the BCG and ICL (Conroy et al. 2007), implying that this basic physical picture can largely explain two significant results from our work without invoking significant bias due to sample selection.

4. The mean BCG+ICL luminosity fraction for our sample decreases monotonically from 65% within $0.1r_{200}$ to 33% within r_{200} . This trend is qualitatively similar to that seen in the stacked sample of Zibetti et al. (2005).

5. Interior to r_{200} , we find that the BCG+ICL optical luminosity fraction is inversely correlated with cluster velocity dispersion. Our mean value of 33% is somewhat larger than one might expect based upon the work of Zibetti et al. (2005), who found a similar luminosity fraction of 32% within a smaller, 500 kpc radius. This difference likely reflects a difference between the systems included in the two studies. For clusters with $\sigma > 750 \text{ km s}^{-1}$, we obtain a mean value of 23% within r_{200} , which is consistent with both the Zibetti et al. (2005) results and simulated BCG+ICL luminosity fractions within r_{200} for rich clusters (Willman et al. 2004).

The authors thank the referee, Stefano Ettori, for excellent suggestions that significantly improved the paper. AHG also thanks Andrey Kravtsov and Yen-Ting Lin for insightful discussions regarding this project. AIZ is supported by NSF grant AST-0206084 and NASA LTSA grant NAG5-11108. DZ acknowledges financial support for this work from a Guggenheim fellowship and NASA LTSA grant 04-0000-0041. AIZ and DZ thank the KITP

for its hospitality and financial support through the National Science Foundation grant PHY99-07949, and generous support from the NYU Physics department and

Center for Cosmology and Particle Physics during their sabbatical there.

REFERENCES

- Aguerri, J. A. L., Gerhard, O. E., Arnaboldi, M., Napolitano, N. R., Castro-Rodriguez, N., & Freeman, K.-C. 2005, *AJ*, 129, 2585
- Arnaud, M., Pointecouteau, E., & Pratt, G. W. 2005, *A&A*, 441, 893
- Bautz, L. P. & Morgan, W. W. 1970, *ApJ*, 162, L149+
- Bertelli, G., Bressan, A., Chiosi, C., Fagotto, F., & Nasi, E. 1994, *A&AS*, 106, 275
- Bertin, E. & Arnouts, S. 1996, *A&AS*, 117, 393
- Blanton, M. R., Hogg, D. W., Bahcall, N. A., Brinkmann, J., Britton, M., Connolly, A. J., Csabai, I., Fukugita, M., Loveday, J., Meiksin, A., Munn, J. A., Nichol, R. C., Okamura, S., Quinn, T., Schneider, D. P., Shimasaku, K., Strauss, M. A., Tegmark, M., Vogeley, M. S., & Weinberg, D. H. 2003, *ApJ*, 592, 819
- Bruzual, G. & Charlot, S. 2003, *MNRAS*, 344, 1000
- Bryan, G. L. 2000, *ApJ*, 544, L1
- Cappellari, M., Bacon, R., Bureau, M., Damen, M. C., Davies, R. L., de Zeeuw, P. T., Emsellem, E., Falcón-Barroso, J., Krajnović, D., Kuntschner, H., McDermid, R. M., Peletier, R. F., Sarzi, M., van den Bosch, R. C. E., & van de Ven, G. 2006, *MNRAS*, 366, 1126
- Cheng, L.-M., Borgani, S., Tozzi, P., Tornatore, L., Diaferio, A., Dolag, K., He, X.-T., Moscardini, L., Murante, G., & Tormen, G. 2005, *A&A*, 431, 405
- Christlein, D. & Zabludoff, A. I. 2003, *ApJ*, 591, 764
- Ciardullo, R., Williams, B. F., Durrell, P. R., Vinciguerra, M., Feldmeier, J. J., Jacoby, G. H., Sigurdsson, S., von Hippel, T., Ferguson, H., Tanvir, N., Arnaboldi, M., Gerhard, O., Aguerri, A., & Freeman, K. C. 2005, *Bulletin of the American Astronomical Society*, 37, 1297
- Conroy, C., Wechsler, R. H., & Kravtsov, A. V. 2007, *ArXiv Astrophysics e-prints*
- De Lucia, G., Kauffmann, G., & White, S. D. M. 2004, *MNRAS*, 349, 1101
- Durrell, P. R., Ciardullo, R., Feldmeier, J. J., Jacoby, G. H., & Sigurdsson, S. 2002, *ApJ*, 570, 119
- Ettori, S. 2003, *MNRAS*, 344, L13
- Ettori, S., Dolag, K., Borgani, S., & Murante, G. 2006, *MNRAS*, 365, 1021
- Feldmeier, J. J., Ciardullo, R., Jacoby, G. H., & Durrell, P. R. 2004a, *ApJ*, 615, 196
- Feldmeier, J. J., Mihos, J. C., Morrison, H. L., Harding, P., Kaib, N., & Dubinski, J. 2004b, *ApJ*, 609, 617
- Fioc, M. & Rocca-Volmerange, B. 1997, *A&A*, 326, 950
- Gastaldello, F., Buote, D. A., Humphrey, P. J., Zappacosta, L., Bullock, J. S., Brighenti, F., & Mathews, W. G. 2006, *ArXiv Astrophysics e-prints*
- Gerhard, O., Arnaboldi, M., Freeman, K. C., Kashikawa, N., Okamura, S., & Yasuda, N. 2005, *ApJ*, 621, L93
- Girardi, M., Borgani, S., Giuricin, G., Mardirossian, F., & Mezzetti, M. 2000, *ApJ*, 530, 62
- Girardi, M., Giuricin, G., Mardirossian, F., Mezzetti, M., & Bosch, W. 1998, *ApJ*, 505, 74
- Gonzalez, A. H., Zabludoff, A. I., & Zaritsky, D. 2005, *ApJ*, 618, 195
- Gonzalez, A. H., Zabludoff, A. I., Zaritsky, D., & Dalcanton, J. J. 2000, *ApJ*, 536, 561
- Hansen, S. M., McKay, T. A., Wechsler, R. H., Annis, J., Sheldon, E. S., & Kimball, A. 2005, *ApJ*, 633, 122
- He, P., Feng, L.-L., & Fang, L.-Z. 2005, *ApJ*, 623, 601
- Kochanek, C. S., White, M., Huchra, J., Macri, L., Jarrett, T. H., Schneider, S. E., & Mader, J. 2003, *ApJ*, 585, 161
- Kravtsov, A. V., Nagai, D., & Vikhlinin, A. A. 2005, *ApJ*, 625, 588
- Krick, J. E., Bernstein, R. A., & Pimbblet, K. A. 2006, *AJ*, 131, 168
- Lin, Y.-T. & Mohr, J. J. 2004, *ApJ*, 617, 879
- Lin, Y.-T., Mohr, J. J., & Stanford, S. A. 2003, *ApJ*, 591, 749
- , 2004, *ApJ*, 610, 745
- McCarthy, I. G., Bower, R. G., & Balogh, M. L. 2006, *ArXiv Astrophysics e-prints*
- Merritt, D. 1984, *ApJ*, 276, 26
- Monaco, P., Murante, G., Borgani, S., & Fontanot, F. 2006, *ArXiv Astrophysics e-prints*
- Moore, B., Katz, N., Lake, G., Dressler, A., & Oemler, Jr., A. 1996, *Nature*, 379, 613
- Moore, B., Lake, G., & Katz, N. 1998, *ApJ*, 495, 139
- Murante, G., Arnaboldi, M., Gerhard, O., Borgani, S., Cheng, L. M., Diaferio, A., Dolag, K., Moscardini, L., Tormen, G., Tornatore, L., & Tozzi, P. 2004, *ApJ*, 607, L83
- Peng, C. Y., Ho, L. C., Impey, C. D., & Rix, H.-W. 2002, *AJ*, 124, 266
- Purcell, C. W., Bullock, J. S., & Zentner, A. R. 2007, *ArXiv Astrophysics e-prints*
- Ramella, M., Bosch, W., Geller, M. J., Mahdavi, A., & Rines, K. 2004, *AJ*, 128, 2022
- Rasmussen, J. & Ponman, T. J. 2006, *ArXiv Astrophysics e-prints*
- Rines, K., Geller, M. J., Diaferio, A., Kurtz, M. J., & Jarrett, T. H. 2004, *AJ*, 128, 1078
- Roussel, H., Sadat, R., & Blanchard, A. 2000, *A&A*, 361, 429
- Rudick, C. S., Mihos, J. C., & McBride, C. 2006, *ApJ*, 648, 936
- Schlegel, D. J., Finkbeiner, D. P., & Davis, M. 1998, *ApJ*, 500, 525
- Sommer-Larsen, J. 2006, *MNRAS*, 369, 958
- Sommer-Larsen, J., Romeo, A. D., & Portinari, L. 2005, *MNRAS*, 357, 478
- Spergel, D. N., Bean, R., Dore, O., Nolta, M. R., Bennett, C. L., Hinshaw, G., Jarosik, N., Komatsu, E., Page, L., Peiris, L., Verde, L., Barnes, C., Halpern, M., Hill, R. S., Kogut, A., Limon, M., Meyer, S. S., Odegard, N., Tucker, G. S., Weiland, J. L., Wollack, E., & Wright, E. L. 2006, *ApJ*
- Valdarnini, R. 2003, *MNRAS*, 339, 1117
- Vikhlinin, A., Kravtsov, A., Forman, W., Jones, C., Markevitch, M., Murray, S. S., & Van Speybroeck, L. 2006, *ApJ*, 640, 691
- White, S. D. M., Navarro, J. F., Evrard, A. E., & Frenk, C. S. 1993, *Nature*, 366, 429
- Willman, B., Governato, F., Wadsley, J., & Quinn, T. 2004, *MNRAS*, 355, 159
- Wu, X.-P., Xue, Y.-J., & Fang, L.-Z. 1999, *ApJ*, 524, 22
- Zabludoff, A. I., Huchra, J. P., & Geller, M. J. 1990, *ApJS*, 74, 1
- Zaritsky, D., Gonzalez, A. H., & Zabludoff, A. I. 2004, *ApJ*, 613, L93
- , 2006, *ApJ*, 638, 725
- Zaritsky, D., Schectman, S. A., & Bredthauer, G. 1996, *PASP*, 108, 104
- Zhang, Y., Finoguenov, A., Boehringer, H., Kneib, J., Smith, G. P., Czoske, O., & Soucaill, G. 2007, *ArXiv Astrophysics e-prints*
- Zibetti, S., White, S. D. M., Schneider, D. P., & Brinkmann, J. 2005, *MNRAS*, 358, 949